DOI: https://doi.org/10.1115/1.4044863

On the mechanism of band gap formation in beams with periodic arrangement of beam-like resonators

O. Serrano, R. Zaera, and J. Fernandez-Saez
Department of Continuum Mechanics and Structural Analysis
University Carlos III of Madrid
Av. de la Universidad 30, 28911 Leganes, Madrid, Spain
Emails: oscar.serrano@uc3m.es, ramon.zaera@uc3m.es, jose.fernandez@uc3m.es

Metastructures made of spring-mass resonators use to present a band gap at the natural frequency of the resonator. This rule cannot be generalized for more complex resonators. This work analyses the case of a metastructure composed by a periodic arrangement of vertical beams rigidly joined to a horizontal beam. The vertical beams work as resonators, and their natural frequencies play a strong role on the band structure of the whole system, however, different to the case with spring-mass resonators. Since this metastructure can be considered as a lattice, Bloch's theorem is applied to the unit cell and a numerical procedure based on the Finite Element Method permits to obtain the dispersion curves. Illustrative results show the influence of the natural frequencies of the horizontal and vertical beams on the band structure.

1 Introduction

In the past decade, the study of metamaterials based on periodic structures has drastically increased in the wave propagation field. The ability of these metastructures in the formation of band gaps and the location of them at the required frequency has caught the attention of many researchers [1, 2].

Among the great variety of metastructures, systems composed by a substrate (plate or beam) and an array of spring-mass resonators periodically joined to it have been commonly investigated [3–5]. Moreover, studies related to systems with beams working as resonators instead of the spring-mass ones have been developed by several authors [2, 6–9].

A metastructure composed by a plate as substrate and a square arrangement of spring-mass resonators joined to it, considered as a lattice structure, was studied by Xiao et al. [3]. The authors showed the evidence of a band gap around the resonant frequency when they vibrate perpendicularly to the plate. Additionally, Sugino et al. [5] stated that the width of this band gap is related to the ratio of the mass of the resonator to the mass of the portion of plate corresponding to the unit cell. A honeycomb arrangement of these spring-mass resonators was studied by Torrent et al. [10]. In this work it was found that the frequency at which the Dirac cone appears depends on their resonant frequency. Hsu [11] studied a plate arranged with stubs working as resonators. The band gaps show up due to the combination of Bragg scattering and resonances of the stubs mechanisms.

A metastructure composed by a beam as substrate of a periodic arrangement of spring-mass resonators was studied by Sugino et al. [4]. In this work, they evidenced again a band gap whose mean value is close to their resonant frequency and its width is related to the ratio of the mass of the resonator to the mass of the portion of beam corresponding to the unit cell. Huang et al. [12] studied a beam with an arrangement of more complex resonators made of inclined trusses joined to conventional spring-mass resonators. Despite of the complexity, the band gaps still appeared around the spring-mass natural frequencies.

In summary, the above works concluded that the band gaps generated by metastructures with spring-mass resonators always exist and appear at the natural frequency of the resonators. However, these represent a idealization slightly away from reality. A real resonator has mass and stiffness distributed along its length and its deformation could not be exclusively transversal to the substrate when the system vibrates. Hence, it is convenient to study a type of resonator that better covers these effects. The metastructure presented in this paper is composed by a beam as substrate and an arrangement of other beams joined to it, working as resonators. Similarly to metastructures with spring-mass attachments, they should show band gaps at the natural frequencies of a clamped-free beam. However, for this kind of resonators the rule stated above cannot be generalized. Xiao et al. [13] showed this exception for a system composed by a beam as substrate of an array of beam-like resonators. The authors suggest that the resonant frequency of the resonators does not necessarily lie in a band gap. Serrano et al. [2] also showed this behavior for a system composed by a plate as substrate and different arrangements of beam-resonators joined to it. In the cited work, the band gaps do not appear at the natural frequencies of the beams working under bending vibration. A brief remark of this singularity on the band gap formation is made on [2, 13]. Thus, in the current work, we give a extended analysis focusing on the role of resonator natural frequencies on the band structure of the whole system. In the following sections, we present a study showing a high influence of the resonant frequencies on the appearance, location, and width of the band gaps in the dispersion curves of the metastructure. For some cases, the beam-like resonators enforce the formation of band gaps at their natural frequencies but, for others, these frequencies just limit the width of the band gaps. The results will show the ability of beam-like resonators to create band gaps due to bending and axial vibration, in contrast to the spring-mass resonators in which the band gap is only created by the axial vibration of the resonator.

The paper is organized as follows. Section 1 provides a brief introduction and Section 2 describes the problem considered in the study. Section 3 provides the methodology used to apply Bloch's theorem to the FEM model of the unit cell. Section 4 presents the wave propagation characteristics of the metastructure and the band gap evolution influenced by the resonant frequencies of the beams within the unit cell. Finally, Section 5 summarizes the main results of the work.

2 Problem formulation

Let us consider a system consisting of an infinite beam parallel to the X axis, and a periodic array of beams perpendicular to the first one and with their lower ends rigidly joined to it. Both the length of the vertical beams and distance between them is equal to L. A scheme of the metastructure is depicted in Fig. 1a. The beams are considered to be slender, thus permitting to use Euler-Bernoulli theory, neglecting the effect of shear strains. Same Young's modulus E and volumetric density ρ are considered for both vertical and horizontal beams. Circular cross-section with distinct diameter for vertical (D_V) and horizontal (D_H) beams is selected. The degrees of freedom of the system are u, w, θ for the horizontal and vertical beams, which can be identified in the representative unit cell, Fig. 1b, u, w being the displacements in X and Z direction, respectively, and θ, the rotation around the out-of-plane axis.

The plane-wave propagation characteristics of the defined metastructure are analyzed in the following sections.

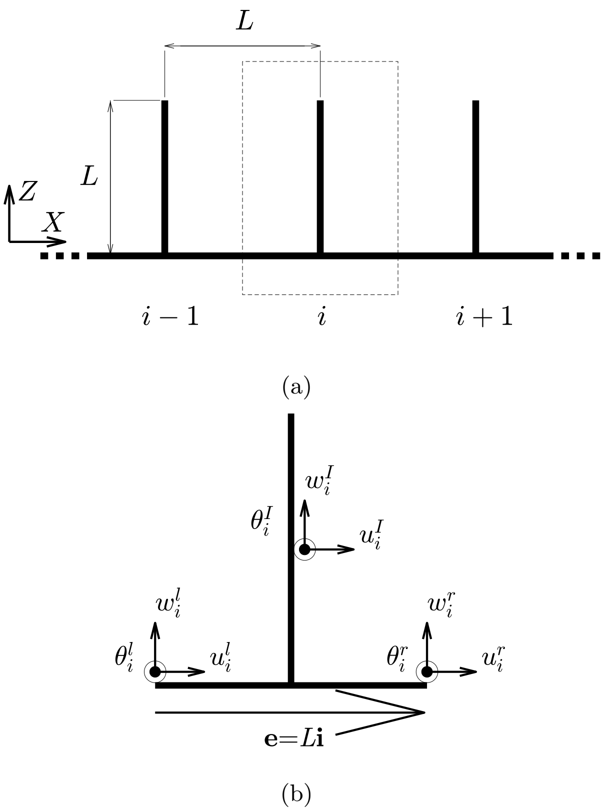

Fig. 1: Lattice structure: (a) Scheme of the metastructure, (b) Unit cell i with degrees of freedom of boundary (left and right) and internal points, and lattice vector $\mathbf{e}$.

3 Numerical Analysis

We are going to apply Bloch's theorem [1, 2] to the representative unit cell (Fig. 1b) which defines the lattice structure. The intrinsic periodicity allows to analyze a single unit cell in order to obtain the dispersive properties of the whole lattice. We have followed an approach based on the FEM model of the unit cell, which has been modeled as two perpendicular beams rigidly joined at the middle point of the horizontal one. Stiffness and mass matrices are built for a two-node Euler-Bernoulli beam element in the classical way [14]. Assuming a plane-wave solution, the equation of motion leads to the following eigenvalue problem written in matrix form as

$$(\mathbf{K} - \omega^2 \mathbf{M})\mathbf{u} = 0, \tag{1}$$

where $\mathbf{K}$ and $\mathbf{M}$ are the global stiffness and mass matrices, respectively, and $\mathbf{u}$ contains the displacements and rotations of the unit-cell nodes. These can be either internal nodes or boundary nodes, shared with the neighboring cells. Bloch's theorem states a constraint condition between the displacements and rotations of the boundary nodes. Let $\mathbf{u}_i^\mathbf{r}$ and $\mathbf{u}_i^\mathbf{l}$ be the displacements and rotations of the right and left boundary nodes (Fig.

1b), respectively, defined by

$$\mathbf{u}_i^\mathbf{r} = \begin{pmatrix} u_i^r \\ w_i^r \\ \theta_i^r \end{pmatrix}, \quad \mathbf{u}_i^\mathbf{l} = \begin{pmatrix} u_i^l \\ w_i^l \\ \theta_i^l \end{pmatrix}. \tag{2}$$

Then, in accordance to Bloch's theorem, $\mathbf{u}_i^\mathbf{r}$ and $\mathbf{u}_i^\mathbf{l}$ have the following relationship

$$\mathbf{u}_i^\mathbf{r} = \mathrm{e}^{\mathrm{i}\mathbf{k}\cdot\mathbf{e}}\mathbf{u}_i^\mathbf{l} = \mathrm{e}^{\mathrm{i}\kappa}\mathbf{u}_i^\mathbf{l}, \tag{3}$$

where $\mathbf{k}$ is the wavevector and $\mathbf{e}$ is the lattice vector defined in Fig. 1b. Focusing the analysis just for wavevectors within the First Brillouin Zone [1], $\kappa = \mathbf{k}\cdot\mathbf{e} \in [0, \pi]$. Hence, the vector $\mathbf{u}$ can be expressed as a function of $\mathbf{u}_i^\mathbf{l}$ and $\mathbf{u}_i^\mathbf{I}$ (of size 3N×1, being N the number of internal nodes) by

$$\mathbf{u} = \begin{Bmatrix} \mathbf{u}_i^\mathbf{r} \\ \mathbf{u}_i^\mathbf{l} \\ \mathbf{u}_i^\mathbf{I} \end{Bmatrix} = \mathbf{T}\mathbf{u}_\mathbf{R}; \mathbf{T} = \begin{bmatrix} \mathrm{e}^{\mathrm{i}\kappa}\mathbf{I}_3 & \mathbf{0}_{3,3\mathrm{N}} \\ \mathbf{I}_3 & \mathbf{0}_{3,3\mathrm{N}} \\ \mathbf{0}_{3\mathrm{N},3} & \mathbf{I}_{3\mathrm{N}} \end{bmatrix}; \mathbf{u}_\mathbf{R} = \begin{Bmatrix} \mathbf{u}_i^\mathbf{l} \\ \mathbf{u}_i^\mathbf{I} \end{Bmatrix}, \tag{4}$$

where $\mathbf{I}_\mathrm{m}$ is the identity matrix of order m and $\mathbf{0}_{\mathrm{m,n}}$ is the zero matrix of size m×n. Introducing Eq. (4) into Eq. (1), and premultiplying by $\mathbf{T}^\mathbf{H}$ (Hermitian transpose of $\mathbf{T}$), we get

$$\mathbf{T}^\mathbf{H}(\mathbf{K} - \omega^2\mathbf{M})\mathbf{T}\mathbf{u}_\mathbf{R} = 0. \tag{5}$$

Finally, the dispersive behavior of the lattice expressed as $\omega = \omega(\kappa)$ can be derived from the solution of the eigenvalue problem given by Eq. (5).

4 Analysis of results

Band structure and mode shapes, derived from the solution of Eq. (5), will be presented for specific mechanical properties. These correspond to steel (Young's modulus $E = 2.1\cdot 10^{11}$ N/m^2, mass density $\rho = 7800$ kg/m^3). The length of the beams is $L = 1$ m, and the diameters of horizontal and vertical beams are $D_H = 0.1$ m and $D_V = 0.15$ m, respectively, for the first analysis that will be presented. Later on, these diameters will be modified in order to analyze their influence on the band structure. In both analyses, the natural frequencies of a beam of length l and diameter d working under clamped-free (hereinafter C−F) or clamped-pinned (hereinafter C−P) boundary conditions are included to clarify their influence in the band structure of the metastructure. The parameters l and d take the corresponding values of the horizontal and vertical beams.

4.1 Dispersion curves and mode shapes

Dispersion curves (Fig. 2a) and shape of modes 3, 4, and 5 at certain wavenumbers (Figs. 2b-2f) are presented.

For mode 3 at $\kappa = 0$, the transverse displacement of the vertical beam, shown in Fig. 2b, fits the first bending mode shape of a C−F beam (leaving aside the rigid-body motion due to the displacement and rotation at the join with the horizontal beam). For the mode 5 at $\kappa = \pi$, the deformation of the vertical beam in Z direction corresponds to the first axial mode shape of a C−F beam (Fig. 2f); regarding the horizontal beam, each half shows transverse displacement which fits the first bending mode of a C−P beam. These evidences suggest the influence of the corresponding natural frequencies on the dispersion curves. It can be verified that frequencies of mode 3 at $\kappa = 0$ and mode 5 at $\kappa = \pi$ at the dispersion curves take the frequency values of the corresponding natural modes discussed above. Hence, Fig. 2a includes the first axial and bending natural frequencies of a C−F beam ($l = L$, $d = D_V$) and the first bending natural frequency of a C−P beam ($l = L/2$, $d = D_H$) in order to show their influence on the dispersion curves. Additionally, the shape of modes surrounding the band gap (modes 3 and 4) at $\kappa = 0$ and $\kappa = \pi$ are shown in Figs. 2b-2e for completeness of the analysis.

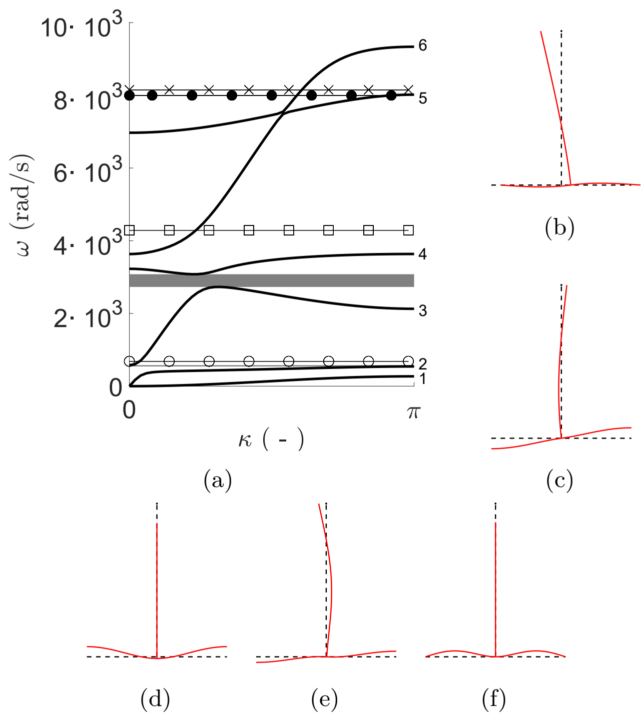

Fig. 2: (a) Dispersion curves (solid lines) and band gaps (gray zones) for $D_V = 0.15$ m, $D_H = 0.1$ m, and $L = 1.0$ m and natural frequencies of C−F beam and C−P beam: ×: $\omega_{1,\mathrm{axial}}^{\mathrm{C-F}}(d = D_V, l = L)$, ∘: $\omega_{1,\mathrm{bending}}^{\mathrm{C-F}}(d = D_V, l = L)$, □: $\omega_{2,\mathrm{bending}}^{\mathrm{C-F}}(d = D_V, l = L)$, •: $\omega_{1,\mathrm{bending}}^{\mathrm{C-P}}(d = D_H, l = L/2)$, (b) Shape of mode 3 at $\kappa = 0$, (c) Shape of mode 3 at $\kappa = \pi$, (d) Shape of mode 4 at $\kappa = 0$, (e) Shape of mode 4 at $\kappa = \pi$, (f) Shape of mode 5 at $\kappa = \pi$.

As mentioned above, other works [4] stated that a band gap appears at the natural frequency of the resonators, which were composed by a spring of stiffness k and a mass m (natural frequency $\omega = \sqrt{k/m}$), vibrating perpendicularly to the beam. Here, as it can be observed in Fig. 2a, the band gaps do not appear around the natural frequencies of a C−F beam nor C−P beam. In this case, when κ tends to π, modes 2 and 5 trend towards these natural frequencies. Frequency of mode 3 at $\kappa = 0$, which shows a bending C−F mode shape of the vertical beam, matches with the first bending frequency of a C−F beam. Frequency of mode 5 at $\kappa = \pi$, which shows an axial C−F mode shape of the vertical beam and a bending C−P mode shape of the horizontal beam, is limited by the first axial frequency of a C−F beam and the first bending frequency of a C−P beam.

From the results, it is clear to see that the natural frequencies play a role in the dispersive behavior. They evidence that the band gaps do not appear around the natural frequencies of the beam-like resonator, at least, for the selected set of mechanical properties.

4.2 Evolution of band structures with the diameter of the resonator

In order to know how the natural frequencies of the resonators, or of the horizontal beam, interfere in the band structure of the system, as found in Fig. 2a for specific mechanical properties, we have performed a parametric analysis varying the diameter of vertical beams D_V, thus inducing changes in both area and inertia of the vertical beam. These modify the bending natural frequencies of the resonator, while keeping the axial ones unchanged. Then the analysis consists in deriving the band structure as a function of D_V, and it has been done for D_V ranging from 0.01 m to 0.3 m, and $D_H = 0.1$ m.

Fig. 3 shows the evolution of the band structures for $D_H = 0.1$ m. The gray zones represent the amplitude of the band gaps at a certain D_V/D_H. The first axial and bending natural frequencies of a C−F beam of length l and diameter d, and the first bending natural frequencies of a C−P beam of length l and diameter d are included in both figures for the mechanical properties specified above.

From Fig. 3 it can be noticed that the axial and bending natural frequencies of a C−F beam and a C−P beam develop a decisive role in the formation of band gaps. For values of D_V close to the lower limit, the bending natural frequencies of a C−F beam pass through the band gaps. This agrees with the hypothesis that a band gap exists at the natural frequency of the resonator, similarly to the behavior of spring-mass resonators attached to a horizontal beam [4]. As D_V increases, the natural frequencies move from creating band gaps around them to limiting their width. The transition of this effect appears around $D_V/D_H = 1$. For values of D_V smaller than D_H, the resonators create band gaps at their bending

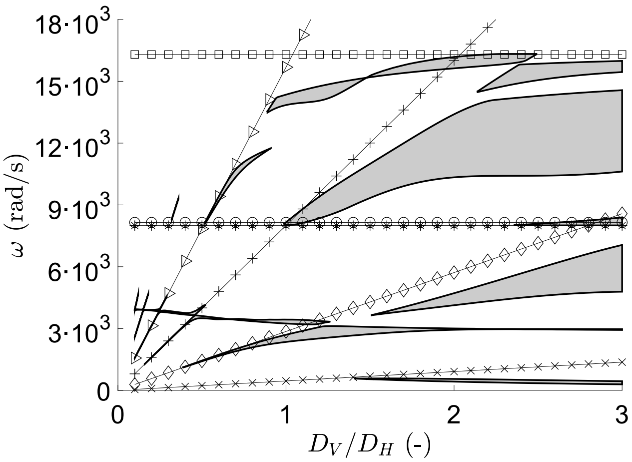

Fig. 3: Evolution of band gaps with D_V/D_H ($D_H = 0.1$ m, and $L = 1.0$ m). ○: $\omega_{1,\text{axial}}^{\text{C−F}}(d = D_V, l = L)$, □: $\omega_{1,\text{axial}}^{\text{C−F}}(d = D_H, l = L/2)$, ∗: $\omega_{1,\text{bending}}^{\text{C−P}}(d = D_H, l = L/2)$, ×: $\omega_{1,\text{bending}}^{\text{C−F}}(d = D_V, l = L)$, ◇: $\omega_{2,\text{bending}}^{\text{C−F}}(d = D_V, l = L)$, +: $\omega_{3,\text{bending}}^{\text{C−F}}(d = D_V, l = L)$, ▷: $\omega_{4,\text{bending}}^{\text{C−F}}(d = D_V, l = L)$.

natural frequencies under C−F boundary conditions. In contrast to this, for values of D_V higher than D_H, the axial natural frequencies under C−F boundary conditions together with the bending ones with C−F and C−P boundary conditions constitute the borders of the band gaps.

5 Conclusions

In this work a metastructure composed by an arrangement of vertical beams rigidly joined to a horizontal beam has been studied. The aim of this work was to analyze the influence of the natural frequencies of the resonators on the formation of band gaps in beams with periodic arrangement of beam-like resonators.

A numerical analysis based on FEM has been done through the application of Bloch's theorem to the unit cell of the metastructure considered as a lattice.

The main finding of the work is that beam-like resonators, in contrast to spring-mass resonators, do not always create band gaps at their natural frequencies, but just for certain values of their mechanical properties. Hence, the rule cannot be generalized. In fact, depending on the ratio of mass and stiffness of the horizontal and vertical beam, the band structure is differently influenced by the natural frequencies of the resonators. For $D_V/D_H < 1$, they create band gaps at their bending natural frequencies under C−F boundary conditions. In contrast, for $D_V/D_H > 1$, natural frequencies due to axial and bending vibration limit the width of the band gaps. For this diameter ratio, bending modes related to the horizontal beam also contribute to this limit.

Acknowledgements

This work was supported by the Ministerio de Economía y Competitividad de España (grant numbers DPI2014-57989-P and BES-2015-073720).

References

[1] Phani, A., Woodhouse, J., and Fleck, N., 2006. “Wave propagation in two-dimensional periodic lattices”. The Journal of the Acoustical Society of America, 119, pp. 1995–2005.

[2] Serrano, Ó., Zaera, R., and Fernández-Sáez, J., 2018. “Band structure analysis of a thin plate with periodic arrangements of slender beams”. Journal of Sound and Vibration, 420, pp. 330–345.

[3] Xiao, Y., Wen, J., and Wen, X., 2012. “Flexural wave band gaps in locally resonant thin plates with periodically attached spring–mass resonators”. Journal of Physics D: Applied Physics, 45, p. 195401.

[4] Sugino, C., Leadenham, S., Ruzzene, M., and Erturk, A., 2016. “On the mechanism of bandgap formation in locally resonant finite elastic metamaterials”. Journal of Applied Physics, 120, 10, p. 134501.

[5] Sugino, C., Xia, Y., Leadenham, S., Ruzzene, M., and Erturk, A., 2017. “A general theory for bandgap estimation in locally resonant metastructures”. Journal of Sound and Vibration, 406, pp. 104 – 123.

[6] Wu, T.-T., Huang, Z.-G., Tsai, T.-C., and Wu, T.-C., 2008. “Evidence of complete band gap and resonances in a plate with periodic stubbed surface”. Applied Physics Letters, 93(11), p. 111902.

[7] Pennec, Y., Djafari-Rouhani, B., Larabi, H., Vasseur, J., and Hladky-Hennion, A., 2008. “Low-frequency gaps in a phononic crystal constituted of cylindrical dots deposited on a thin homogeneous plate”. Physical Review B, 78(10), p. 104105.

[8] Xiao, Y., Wen, J., Huang, L., and Wen, X., 2013. “Analysis and experimental realization of locally resonant phononic plates carrying a periodic array of beam-like resonators”. Journal of Physics D: Applied Physics, 47(4), p. 045307.

[9] Qureshi, A., Li, B., and Tan, K., 2016. “Numerical investigation of band gaps in 3d printed cantilever-in-mass metamaterials”. Scientific reports, 6, p. 28314.

[10] Torrent, D., Mayou, D., and Sanchez-Dehesa, J., 2013. “Elastic analog of graphene: Dirac cones and edge states for flexural waves in thin plates”. Physical Review B, 87.

[11] Hsu, J.-C., 2011. “Local resonances-induced low-frequency band gaps in two-dimensional phononic crystal slabs with periodic stepped resonators”. Journal of Physics D: Applied Physics, 44, p. 055401.

[12] Huang, H.-H., Lin, C.-K., and Tan, K.-T., 2016. “Attenuation of transverse waves by using a metamaterial beam with lateral local resonators”. Smart Materials and Structures, 25, p. 085027.

[13] Xiao, Y., Wen, J., Wang, G., and Wen, X., 2013. “Theoretical and experimental study of locally resonant and bragg band gaps in flexural beams carrying periodic arrays of beam-like resonators”. Journal of Vibration and Acoustics, 135(4), p. 041006.

[14] Bauchau, O. A., and Craig, J. I., 2009. Euler-Bernoulli beam theory. Springer Netherlands, Dordrecht.